Calculations of SAR around Implanted Cardiac Pacemaker Induced by Wireless Radio Terminal

Relation between Positions of Implanted Cardiac Pacemaker and Wireless Radio Terminal

Kazuyuki Saito[1,2], Soichi Watanabe[1]
[1]National Institute of Information and Communications Technology
Tokyo, Japan

Yuta Endo[2], Masaharu Takahashi[2], and Koichi Ito[2]
[2]Chiba University
Chiba, Japan

Abstract— **Recently, electromagnetic interference (EMI) of an implanted pacemaker induced by a mobile radio terminal has been investigated. However, there are few studies of specific absorption rate (SAR) around the pacemaker induced by the mobile radio terminal. In this paper, the relation between position of pacemaker model embedded into the torso model, wireless radio terminal model and SAR has been investigated. As a result of calculations, possibilities of increasing the SAR were observed in some cases.**

Keywords-specific absorption rate; implanted cardiac pacemaker; mobile radio terminal; finite difference time domain method; torso model

I. Introduction

The implanted cardiac pacemaker is one of the medical devices for cardiac diseases such as irregular heartbeat, ventricular fibrillation, etc. and is implanted in the chest of patient (Fig. 1). Recently, electromagnetic interference (EMI) of an implanted pacemaker with a mobile radio terminal has been investigated [1]-[3]. Based on these studies, national authorities have recommended that a mobile radio terminal should be kept 22 cm from the pacemaker in Japan [4]. Meanwhile, SAR distribution in the body especially around the pacemaker, when the mobile radio terminal closes to chest of the pacemaker holder, has to be considered (Fig. 2). In this study, the SAR distributions around the pacemaker model embedded into a rectangular parallelepiped torso model due to a mobile radio terminal model were calculated.

II. Numerical Model

Figure 3 shows a planar inversed F antenna with metallic case, which simulates mobile radio terminal, and its calculated reflection coefficient at the feeding point. The antenna operates at 2 GHz and the output power is 0.25 W. Figure 4 shows a pacemaker model implanted in a human torso model. This model is the same as the model in ref. [5]. Here, the pacemaker housing has a dimension of $40\times30\times6$ mm^3, and the lead wire has a diameter of 2 mm, and a length of 240 mm. The connector between the pacemaker housing and the lead wire has a 2 mm gap. Figure 5 shows the arrangements of the torso model and the mobile radio terminal model. The torso is simulated as a rectangular parallelepiped whose electrical properties are the same as the human muscle [6]. The antenna is located in two cases, namely in z (Fig. 5(a)) and x (Fig. 5(b)) directions. Figure 6 shows scanning area of the feeding point. In this paper, in order to find the worst case (position of the mobile radio terminal model and pacemaker model) under some assumptions, the mobile radio terminal model will be scanned in the scanning area. Here, the coordinate origin in the scanning area is the gap between the pacemaker housing and the lead wire. The scanning area is enlarged until the SAR values become sufficiently low at their periphery.

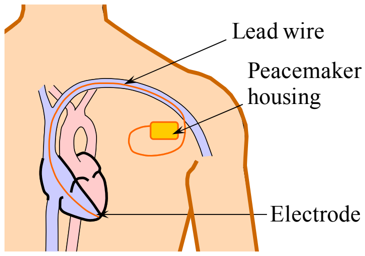

Figure 1. Implanted cardiac pacemaker.

Figure 2. Supposed situations.

TABLE I
PARAMETERS FOR FDTD CALCULATIONS

Cell size [mm]	Δx =2.0, Δy =1.0, Δz =2.0
Analytical space $x \times y \times z$ [cell]	$400\times400\times400$
Absorbing boundary condition	PML (8 layers)

The SAR values are calculated when the feeding point met the grid point of the scanning area by following definition:

$$\mathrm{SAR} = \frac{\sigma}{\rho} E^2 \quad [\mathrm{W/kg}] \tag{1}$$

where σ is the conductivity of the biological tissue [S/m], ρ is the density of the biological tissue [kg/m^3], and E is the electric field (rms) [V/m]. In order to calculate the SAR values in each position, finite-difference time-domain (FDTD) method [7] was employed. Table 1 shows parameters for FDTD calculations.

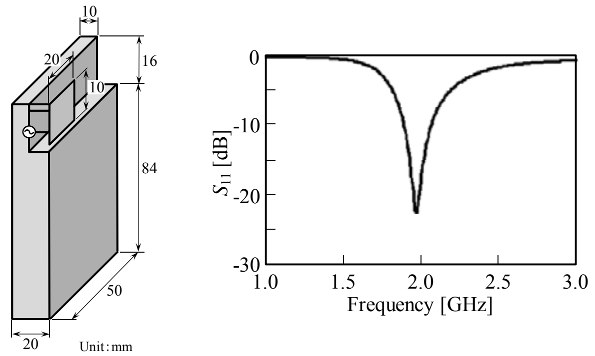

Figure 3. Mobile radio terminal model.

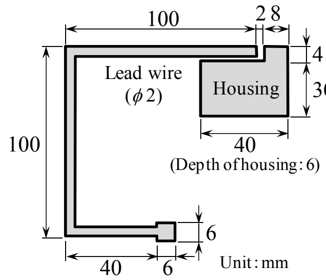

Figure 4. Pacemaker model.

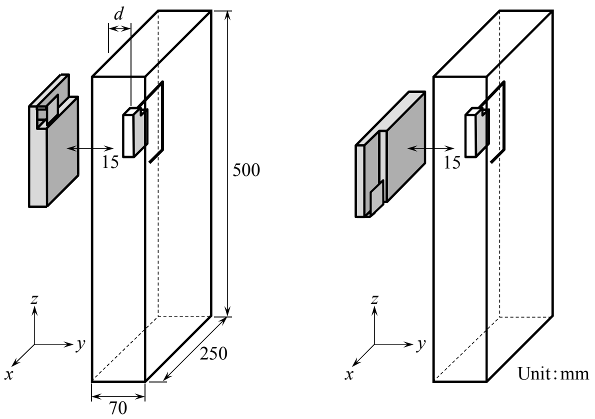

(a) Antenna direction: z (b) Antenna direction: x

Figure 5. Arrangements of torso model and mobile radio terminal model.

III. CALCULATED RESULTS

Figure 7 shows the calculated 10-g averaged SAR in the scanning area, when depth of the pacemaker model d =14 mm. From Fig. 7(a), maximum 10-g averaged SAR appears on the origin of scanning area, in the antenna direction z. On the other hand, in Fig. 7(b), the maximum 10-g averaged SAR is observed at x =10 mm, z =-30 mm. This is a position that the lead wire of x-direction (longer part) overlapped almost center of the metallic case of mobile radio terminal model. In addition, both maximum values of 10-g averaged SARs are same as 1.36 W/kg.

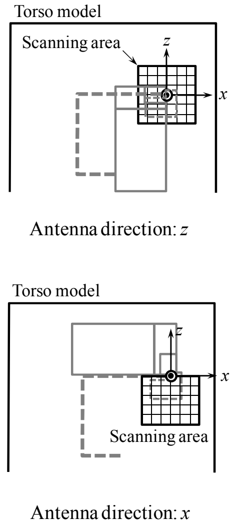

Figure 6. Scanning area of the mobile radio terminal model.

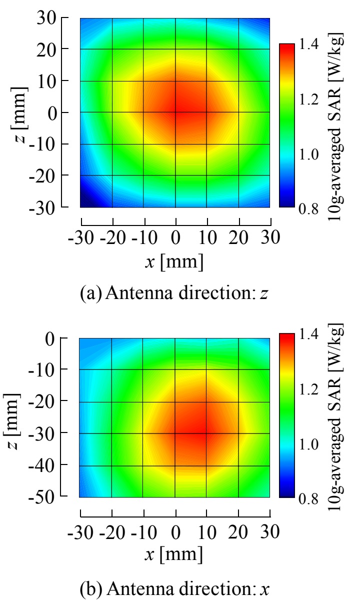

Figure 7. Calculated 10-g averaged SARs. The value of each crossing point corresponds the maximum 10-g averaged SAR in the calculated region, when the feeding point of the wireless radio terminal model was placed on this crossing point.

Table 2 shows comparison of the SAR values between with and without the pacemaker model, where the maximum 10-g averaged SAR value was observed. From the results, in the case of embedding the pacemaker model, the maximum value of 10-g averaged SAR is 30 % larger than that of without pacemaker model.

Figure 8 shows the SAR distributions around pacemaker model in both antenna directions. Here, SAR observation plane is *x*-*z* plane at the surface of the pacemaker housing (*y* =13 mm). The positions of wireless radio terminal model and pacemaker model are the points where the maximum 10-g average SAR was observed in Figs. 7 (a) and (b). From Fig. 8 (a), in the case of antenna direction *z*, high SAR region is observed at border of pacemaker housing and the region, where is the metallic case of the mobile radio terminal model faced (around *x* = -30 mm, *z* = -70 mm). Moreover, from Fig. 8 (b), in the case of antenna direction *x*, high SAR region is also observed at border of pacemaker housing and around the lead wire. They are because of the concentrate on electric field around the conductor.

In addition, SAR distributions under various implanted depth "*d*" are presented in Fig. 9. Here, the observation line is *y*-axis at *x* = -12 mm, *z* = -19 mm (center of pacemaker housing). According to Fig. 9, standing waves are observed between the torso surface and pacemaker model in all cases.

Figure 10 shows one of the examples of electric field distributions around the pacemaker model. From the results, it is observed that the dominant components of standing waves are *x* and *z*. The detail mechanism of the standing wave should be analysed as our further study.

IV. Conclusions

According to the results, the SAR around the conductor, which is implanted in the human body, increased. It is confirmed in [8] as well as our results. In fact, 10-g averaged SAR has been limited in less than 2 W/kg by the guideline on human exposure to electromagnetic fields in Japan. In addition, when the conductors were implanted into the human body, the guideline indicated that the possibility of the exposure below the guideline value might cause a local heating. Thus, the guideline value (i. e. 2 W/kg) was not applied in this case. However, as increasing number of pacemaker user, such a case must be applied to the guideline [9]. Therefore, the influences on SAR by the implanted conductors have to be investigated in detail [10].

Acknowledgment

The authors would like to thank Mr. Watanabe and Mr. Haga for their valuable help for numerical calculations.

TABLE II
Calculated SAR Values with and without Pacemaker Model

	Pacemaker model	
	with	without
10-g averaged SAR [W/kg]	1.36	1.04

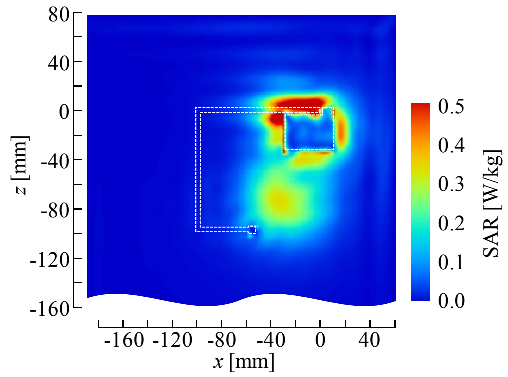

(a) Antenna direction: *z*

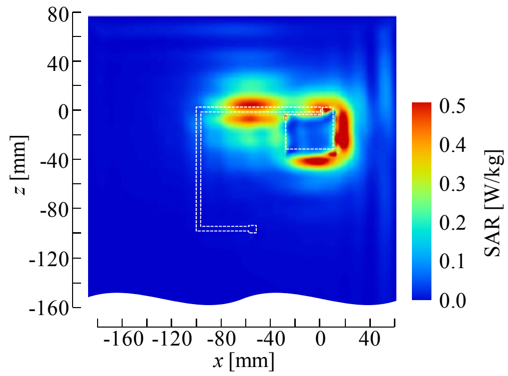

(b) Antenna direction: *x*

Figure 8. Calculated SAR distributions.

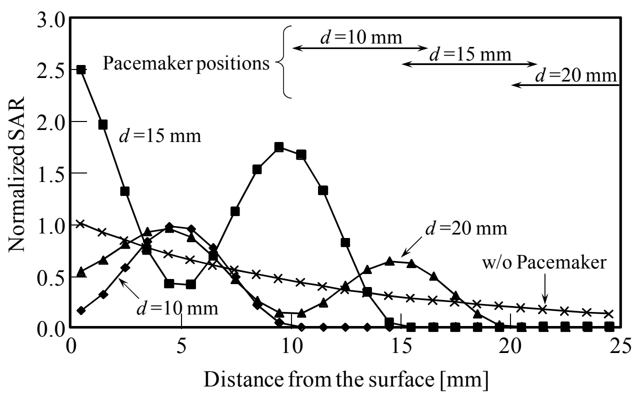

Figure 9. SAR profiles on *y* -axis at *x* =-12 mm, *z* =-19 mm (center of pacemaker housing). The values are normalized by maximum value of "without pacemaker model".

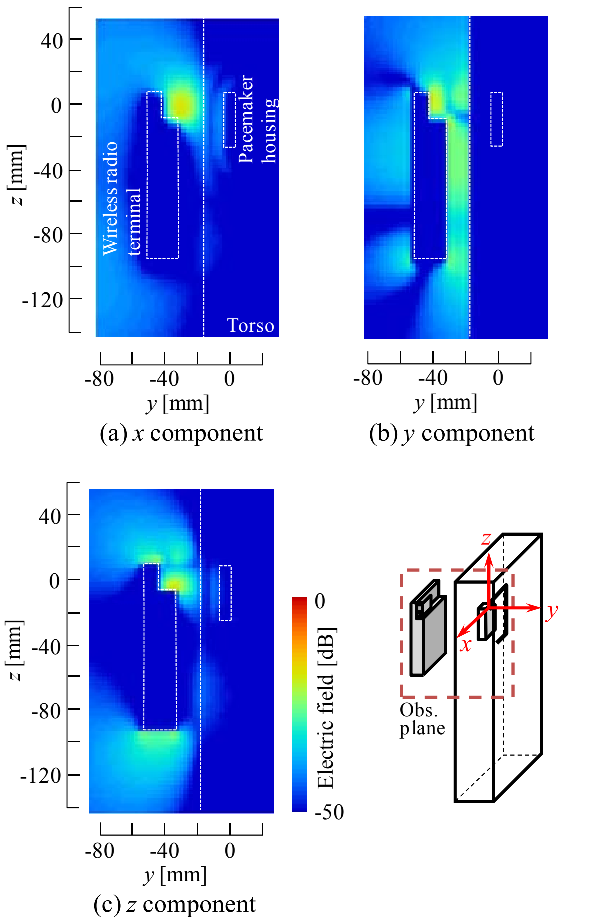

Figure 10. Calculated electric field distributions.

REFERENCES

[1] S. Stefan, LO. Fichte, and S. Dickmann, "EMC Modelling of Cardiac Pacemakers," in Electromagnetic Compatibility, 2007, -EMC Zurich 2007, 18th International Zurich Symposium, Sep. 2007.

[2] S. Hille, KF. Eichhorn, and KH. Gonschorek, "Determination of the interference voltage in implantable medical devices with bipolar electrodes," in Electromagnetic Compatibility -EMC Europe 2008 International Symposium, Sep. 2008.

[3] S. Schenke, F. Sabath, M. Clemens, and S. Dickmann, "Electromagnetic Interference Coupling into Cardiac Pacemaker Electrodes," in Electromagnetic Compatibility -EMC Europe 2008 International Symposium, Sep. 2008.

[4] "Guidelines on the Use of Radio communication Equipment such as Cellular Telephones -Safeguards for Electronic Medical Equipment- ," EMC Conference Japan, Electromagnetic Medical Equipment Study Group, 1997.

[5] J. Wang, O. Fujiwara, and T. Nojima, "A model for predicting electromagnetic interference of implanted cardiac pacemakers by mobile telephones," IEEE Transactions on Microwave Theory and Techniques, vol. 48, no. 11, pp. 2121-2125, Nov. 2000.

[6] C. Gabriel, "Compilation of the dielectric properties of body tissues at RF microwave frequencies," Brooks Air Force Technical Report AL/OE-TR-1996-0037, 1996.

[7] K. S. Yee, "Numerical solution of initial boundary value problems involving Maxwell's equation in isotropic media," IEEE Transactions on Antennas and Propagations, vol. AP-14, no. 3, pp. 302-307, May 1966.

[8] H. Virtanen, J. Huttunen, A. Toropainen, and R Lappalaiainen, "Interaction of mobile phones with superficial passive metallic implants," Physics in Medicine and Biology, vol. 50, pp. 2689-2700, 2005.

[9] C. R. Roy, "Rapporteur report: ICNIRP international workshop on EMF dosimetry and biophysical aspects relevant to setting exposure guidelines," Health Phyics, vol. 92, no. 6, pp. 658- 667, 2007.

[10] International Commission on Non-Ionizing Radiation Protection, "Exposure to high frequency electromagnetic fields, biological effects and health consequences (100 kHz-300 GHz) - review of the scientific evidence and health consequences," 2009.